J Intell Manuf (2011) 22:607–617
DOI 10.1007/s10845-009-0323-5

Surface roughness monitoring application based on artificial neural networks for ball-end milling operations

G. Quintana · M. L. Garcia-Romeu · J. Ciurana

Received: 21 May 2009 / Accepted: 25 September 2009 / Published online: 16 October 2009

Abstract Surface roughness plays an important role in the performance of a finished part. The roughness is usually measured off-line when the part is already machined, although in recent years the trend seems to have been to focus on online monitoring. Measuring and controlling the machining process is now possible thanks to improvements and advances in the fields of computers and sensors. The aim of this work was to develop a reliable surface roughness monitoring application based on an artificial neural network approach for vertical high speed milling operations. Experimentation was carried out to obtain data that was used to train the artificial neural network. Geometrical cutting factors, dynamic factors, part geometries, lubricants, materials and machine tools were all considered. Vibration was captured on line with two piezoelectric accelerometers placed following the X and Y axes of the machine tool.

Keywords Ball end mill · Cutting parameters · Surface roughness · Process monitoring · Neural network modeling

Nomenclature

Ae	Radial depth of cut (mm)
Ap	Axial depth of cut (mm)
C.L.A.	Center line average
Cs	Cutting section (mm^2)
f	Feed rate (mm/ min)
ft	Tooth passing frequency (Hz)
fs	Sampling frequency (Hz)
fz	Feed per tooth (mm/z)
h	Surface crest height (mm)
H	Material hardness (HRC)
hx, hy	High frequency vibration amplitude in X and Y axes
K	Power coefficient
Lm	Length of measurement
lx, ly	Low frequency vibration amplitude in X and Y axes
MQL	Minimum quantity of lubricant
MRR	Material removal rate (mm^3/min)
mx, my	Medium frequency vibration amplitude in X and Y axes
N	Spindle speed (rpm)
O	Cutting tool overhang (mm)
P	Power required (P)
R	Cutter radius (mm)
Ra	Roughness average (μm)
Rat	Theoretical roughness average (μm)
tdx, tdy	Temporal domain vibration amplitude in X and Y axes
tpx, tpy	Tooth passing frequency vibration amplitude in X and Y axes
Vc	Cutting speed (m/min)
W	Tool wear
y	Vertical deviation from the nominal surface
Z	Number of teeth

G. Quintana
ASCAMM Technology Centre, Barcelona, Spain
e-mail: gquintana@ascamm.com

M. L. Garcia-Romeu · J. Ciurana (✉)
Mechanical Engineering and Industrial Construction Department, University of Girona, Girona, Spain
e-mail: quim.ciurana@udg.edu

Introduction

Machining is applied to a wide range of materials to create a great variety of geometries and shapes, with hardly

any complexity restrictions. Typical workpiece materials are: aluminium alloys, cast iron, titanium, austenitic stainless or hardened steel, copper, carbon graphite, as well as plastic, wood and plastic composites. Machined components can be either simple forms with planes and round shapes or complex shapes. In the latter case, two types of surface are usually defined: ruled surfaces (e.g., for blades) and sculptured surfaces or free-form surfaces (e.g., for moulds and dies). This enormous number of combinations is able to meet the specific manufacturing requirements of a wide range of manufacturing industries, such as the automotive, the aerospace or the die and mould industries (López et al. 2008).

There has been constant innovation and technical advances in all fields of manufacturing systems during the last few years. New technologies have been introduced in the market and new concepts in metal cutting such as high speed machining (HSM) have been developed.

The term 'High Speed Machining' has been used for many years to describe end milling with small diameter tools at high rotational speeds. The process was first applied in the aerospace industry for the machining of light alloys. The mould and die industry then began to use the technology for the production of components, including those manufactured from hardened tool steels. This was only made possible by advances in machine tools, cutting tools and CAD/CAM systems (Dewes and Aspinwall 1997).

Surface properties play an important role in the performance of a finished part. They have an enormous influence on features such as dimensional accuracy, friction coefficient and wear, thermal and electric resistance, fatigue limit, corrosion, post-processing requirements, appearance and cost. Surface roughness is usually measured off-line when the part is already machined (Groover 2004) and is a widely used index of product quality and a technical requirement for mechanical products (Benardos and Vosniakos 2003).

A lot of research has been focused on surface generation to understand the process and provide the knowledge necessary to guarantee surface quality before the start of the metal removal operation. In Martellotti (1941, 1945) studied the process from a mathematical point of view to show that the cutting tool path is a trochoidal arc for peripheral milling operations. Later, Quintana et al. (2010) studied the influence of the geometric characteristics of a ball end mill cut on the theoretical surface roughness obtained. Thomas et al. (1996) analyzed the effect of tool vibration on surface roughness for lathe dry turning processes. Abouelatta and Mádl (2001) studied the relationship between tool life, surface roughness and vibration while taking into account cutting speed, feed rate, depth of cut, tool nose radius, tool overhang and the acceleration, among other parameters in radial and feed directions. Grzesik (2008) studied the influence of tool wear on surface roughness in hard turning operations. Ghani and Choudhury (2002) followed an analogous approach using vibration signals to verify surface finish based on tool wear evolution. Risbood et al. (2003) used neural networks to predict surface finish in turning processes considering tool-holder vibration level. The usefulness of an artificial neural network approach has been demonstrated in several fields (Ciurana et al. 2009; Brinksmeier et al. 2006; Chukwujekwu Okafor and Adetona 1995; Markopoulos et al. 2008; Sharma et al. 2008). Correa et al. (2009, 2008) show how effectively Bayesian networks and artificial neural networks predict surface roughness in high-speed machining. Brezocnik and Kovacic (2003) proposed the use of a genetic algorithm approach to predict surface roughness in end milling. Samanta et al. (2008) used soft computing and computational intelligence techniques to model surface roughness in end milling processes featuring multiple regression analyses, artificial neural networks and adaptive neuro-fuzzy inference systems.

In Benardos and Vosniakos (2003) published a review of the state of the art of surface roughness prediction in machining operations. They provided an extensive study of the main research lines and classified the different approaches after considering those based on machining theory, experimental investigation, experimental design and artificial intelligence.

Alongside the various methodologies and strategies adopted by researchers to study surface roughness generation and the finishing techniques applied in industry, several standards have been developed. ISO-4287 and ISO-4288 are both to do with dimensional and geometrical product specification and verification, and focus mainly on surface texture.

Present systems seem to focus on monitoring processes by measuring and controlling the surface roughness (Tsai et al. 1999; Chen and Lou 2000; Huang and Chen 2003; Chang 2007; Zhang et al. 2007). This online monitoring is possible due to improvements and advances in computers and sensor fields.

The purpose of this research is to develop a reliable surface roughness monitoring application based on artificial neural network models for ball end mill finishing operations. As surface roughness can only be evaluated out-of-process, it seems necessary to introduce in-process solutions to control the surface generation process and avoid the need to scrap unacceptable parts once the part is finished and time and energy have been spent on it. A monitoring approach allows lack of quality to be detected as soon as it occurs and the cutting parameters to be modified, or the operation interrupted and the process reconsidered or redefined. The proposed modeling approach captures the vibrations that occur during the metal removal operation with the help of two piezoelectric accelerometers and calculates the current in-process surface roughness average (Ra) parameter. It looks at the cutting parameters and applies the neural network developed. The roughness average parameter (Ra) has been chosen as it is the most widely

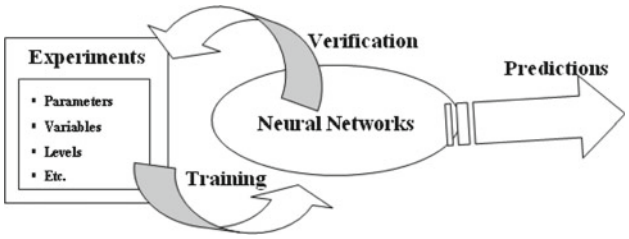

Fig. 1 Methodology schematically represented

used parameter of surface quality evaluation in present-day manufacturing.

The methodology followed to achieve this objective consisted of the following steps: first, experiments were performed, then the neural network was built, trained and verified, and finally it was introduced in the module to monitor surface roughness. Figure 1 presents a schematic representation of the methodology. As the application presented in this paper is based on artificial neural network modeling, a certain amount of information or experience is required to train the network. For this reason it was necessary to carry out experiment with the aim of collecting experience with which to feed and train the artificial neural network for surface roughness predictions.

The paper is structured as follows: Sect. 2 explains the experimental procedure followed to obtain the data used to feed the neural network for surface roughness prediction; Sect. 3 introduces the neural network developed; Sect. 4 shows the surface roughness monitoring platform implemented; and finally, conclusions are summarized in Sect. 5.

Experimental procedure and data collection

Surface roughness is a parameter which refers to the small, finely spaced deviations from the nominal surface determined by the material's characteristics and the process that formed the surface. It can be defined as the average of the vertical deviations from the nominal surface over a specified surface length. In accordance with the ISO 4287:1999 standard, an arithmetic average is generally used, based on the absolute values of the deviations, as shown in Eq. 1 , and the roughness value is referred to by the term average roughness (Groover 2004).

$$\mathrm{Ra} = \int_0^{\mathrm{Lm}} \frac{|y|}{\mathrm{Lm}} dx \tag{1}$$

where Ra is the arithmetic mean value of roughness also known as the center line average (C.L.A.); y is the vertical deviation from the nominal surface converted to an absolute value; and Lm is the specified distance over which the surface deviations are measured.

It is no easy task to identify the process parameters that yield the required product quality by defining surface roughness, while at the same time maximizing the performance of the manufacturing process. Operators usually select conservative combinations of cutting parameters. The set of parameters that influences surface roughness and has motivated researchers has been compiled by Benardos and Vosniakos (2003) in a fishbone diagram that considers machining parameters such as process kinematics, cooling fluid, stepover, depth of cut, tool angle, feed rate and cutting speed; cutting tool properties such as tool material, run-out errors, tool shape and nose radius; workpiece properties such as length, diameter and hardness; and cutting phenomena such as cutting force variation, friction in the cutting zone, chip formation, vibration and acceleration. The interactions among these factors are complex and make it difficult to understand the cause-effect relationships necessary to implement surface roughness models.

The experiments were designed taking into account the majority of parameters that affect surface roughness presented in Benardos and Vosniakos (2003). This would permit the effects of the main factors to be captured and evaluated and a reliable artificial neural network to be implemented. Such a network would be able to calculate the surface roughness generated given a certain combination of cutting characteristics from among all the possibilities available.

The experiments consisted of a simple raster metal removal operation along the machine tool's Y axis. Spindle speed (N), feed rate (f), feed per tooth (fz), axial and radial depths of cut (Ap and Ae) and the type of lubricant used (dry machining or minimum quantity of lubricant (MQL)) were considered. The experimental design aimed to evaluate the wide range of cutting parameters that influence surface roughness generation (see Fig. 2). The parameters used in the experiments were sometimes quite aggressive for the cutting tool, especially in the case of high cutting speed (Vc) values. Despite not being useful to industry due to the reduction in tool life this would entail, for this research it was useful to obtain information about the surface roughness generated by considering a large enough number of parameter combinations. A total of 250 experiments were designed and performed, with five full factorial series of 50 experiments. Cutting parameters and levels are summarized in Table 1. In all series the spindle speed was measured at 10 levels from 6,000 to 24,000 rpm with an increase of 2,000 rpm at each level.

Two series of 50 experiments were carried out, first in dry machining conditions and then with an application of MQL, at a constant feed of 0.075 mm/tooth and a radial depth of cut of 0.4 mm (as suggested by the cutting tool provider in the cutter tables). The experiments were performed at varying spindle speeds (S) and axial depths of cut (Ap) and followed a full factorial design with the levels shown in Table 1. As

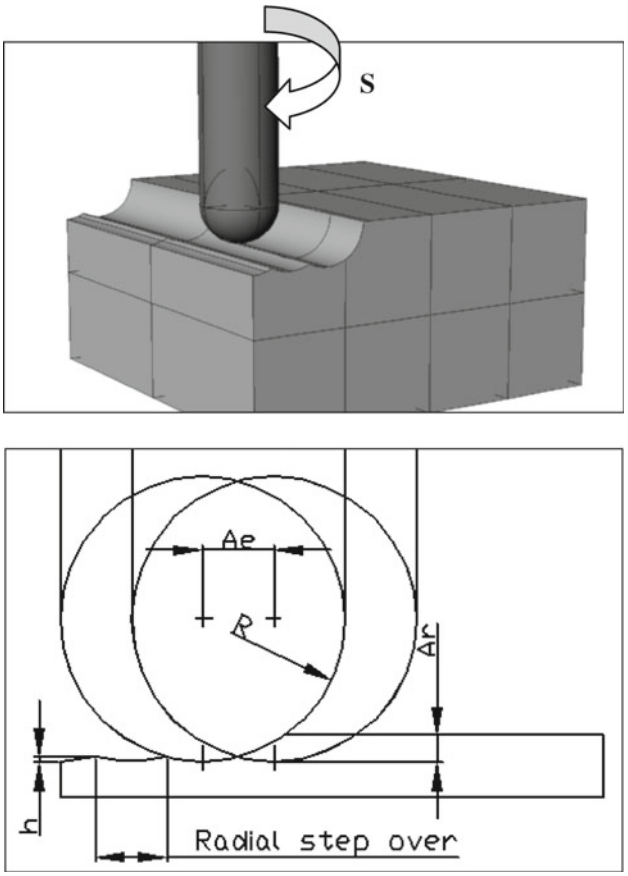

Fig. 2 Surface roughness generation in a vertical ball end milling operation

the frontier between a stable and an unstable cut is shown as combinations of spindle speeds and the axial depths of cut in stability lobe diagrams, the influence of these two cutting parameters was taken into consideration. The radial depth of cut variation was also considered in the third series of 50 experiments, with varying spindle speed (S) and radial depth of cut (Ae) following a full factorial series with the levels shown in Table 1. Other factors analyzed were the feed rate (f) and the feed per tooth (fz), which both affect chip generation and the cutting force. The fourth series of 50 experiments was carried out with a constant radial depth of cut of 0.4 mm and an axial depth of cut of 0.24 mm, as suggested in the

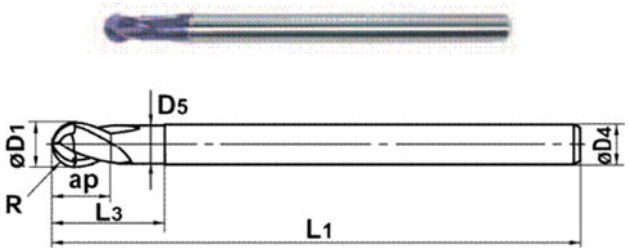

Fig. 3 Schematic representation of the Mitsubishi VC2PSB cutter.

Table 2 Geometric characteristics of the Mitsubishi VC-2PSB cutter

L_1	Overall length (mm)	90
L_3	Neck length (mm)	16
ap	Length of cut (mm)	12
R	Radius of ball nose (mm)	4
D_1	Diameter (mm)	8
D_3	Neck diameter (mm)	7.85
D_4	Shank diameter (mm)	8
Z	Number of teeth	2

cutting tool provider tables. Several levels of feed per tooth (fz) were considered and the feed rate was calculated in Eq 2. Finally, in the fifth series of 50 experiments the tool radius variation was considered by testing Mitsubishi VC-2PSB ball end mill cutting tools of 4, 6, 8, 10 and 12 mm in diameter. This solid cutter has two cutting edges and a regular pitch and helix angle. Figure 3 and Table 2 show the geometric characteristics of the 4 mm radius cutter.

The milling center used to perform the experiments was a Deckel-Maho 105Vlinear three axis vertical high speed machine center with a Heidenhain iTNC 530 control. The material used was quenched steel 1.2344, an analogue of AISI H13 with a hardness of 52–54 HRC, very common in the die and mould industry. PowerMill software was used to generate the CAM G-code.

Labview^{TM} was used to develop a data acquisition platform to acquire and analyze the vibrations occurring in the X and Y axes. Current vibration was obtained with two unidirectional piezoelectric accelerometers, one placed on the spindle (see Fig. 4) and the other on the table following

Table 1 Experimentation parameters

Parameters	Units	Levels									
		1	2	3	4	5	6	7	8	9	10
Spindle speed	rpm	6,000	8,000	10,000	12,000	14,000	16,000	18,000	20,000	22,000	24,000
Radial depth of cut	mm	1.0	0.8	0.6	0.4	0.2					
Tool radius	mm	2	3	4	5	6					
Axial depth of cut	mm	0.10	0.14	0.19	0.24	0.29					
Feed per tooth	mm/z	0.150	0.125	0.100	0.075	0.050					

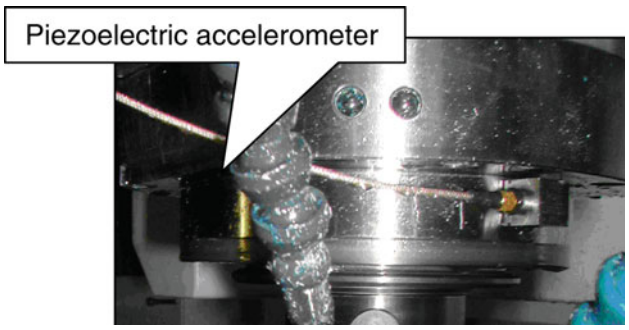

Fig. 4 Piezoelectric accelerometer located in the machine tool spindle

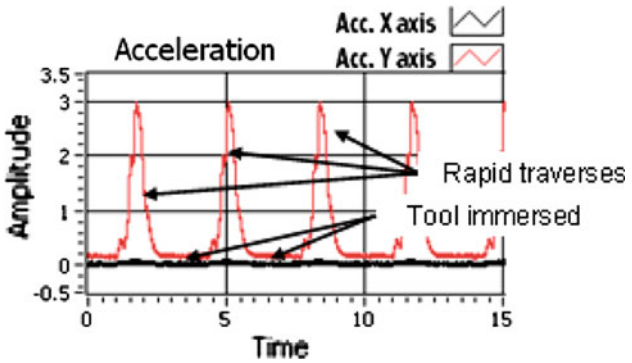

Fig. 5 Accelerations captured by the accelerometers

the corresponding axes. Figure 5 is shows an example of the vibrations captured by the two accelerometers, and it is possible to observe the rapid traverses along the Y axis of the machine tool. Between the rapid traverses, where acceleration is maximum and the tool is immersed in the workpiece, removing material, the machining operation is effective. The sampling frequency (fs) used was 10 kHz. It is also possible to observe the rapid traverses of the table between the effective metal removal passes when the machined surface is generated.

Once the experiments had been performed, surface roughness was measured with a Mitutoyo SV-2000N2 roughness tester. The evaluation length was 7.002 mm and a nominal 2μm stylus tip was used at a speed of 2 m/s, together with a 0.75 mN static stylus force, to obtain 2,334 surface points.

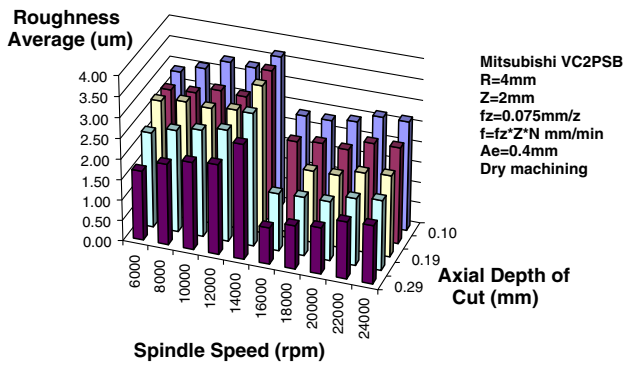

Fig. 7 Surface roughness average considering Ap vs. *N* variations and dry machining

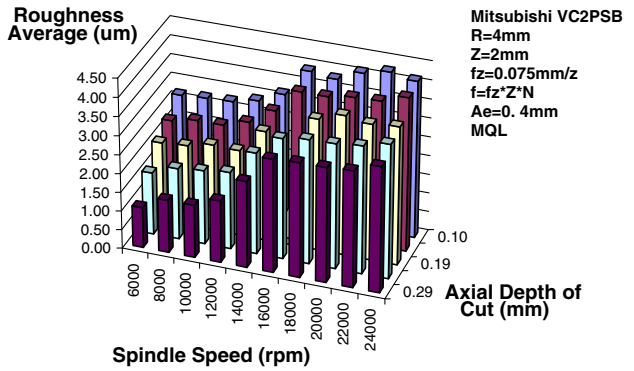

Fig. 8 Surface roughness average considering Ap vs. *N* variations and MQL

Figure 6 shows one of the profiles obtained with the roughness tester.

Figures 7, 8, 9, 10 and 11 present the surface roughness averages obtained for each experiment in the five full factorial series of 50 experiments. The first two series correspond to the Ra as variations of spindle speed vs. axial depth of cut, with two different cooling systems, one in dry machining (Fig. 7) and the other using MQL (Fig. 8). Figure 9 shows the Ra obtained when variations in the radial depth of cut are considered along the machine tool spindle speed range in dry machining. Figure 10 presents the results obtained when variations in feed per tooth vs. spindle speed are considered,

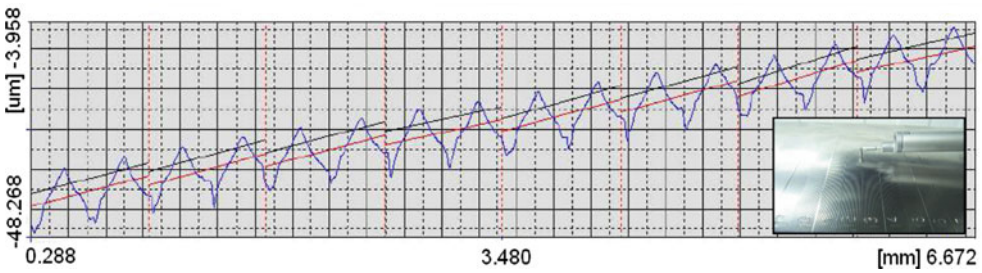

Fig. 6 One of the surface profiles measured with the roughness tester

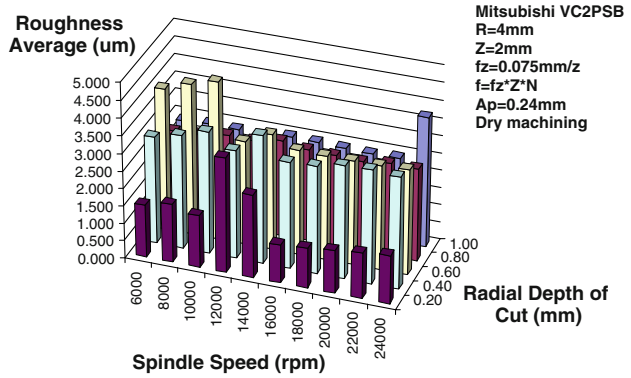

Fig. 9 Surface roughness average considering Ae vs. *N* variations

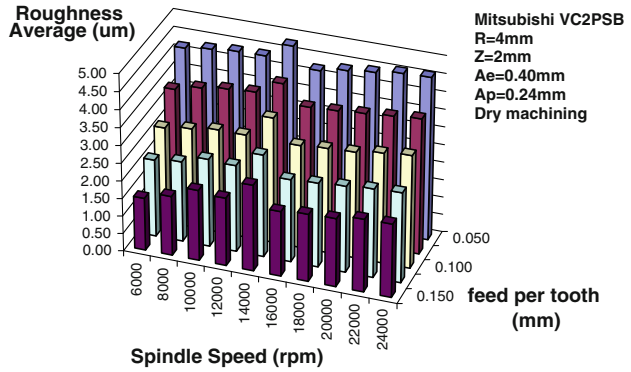

Fig. 10 Surface roughness average considering fz vs. *N* variations

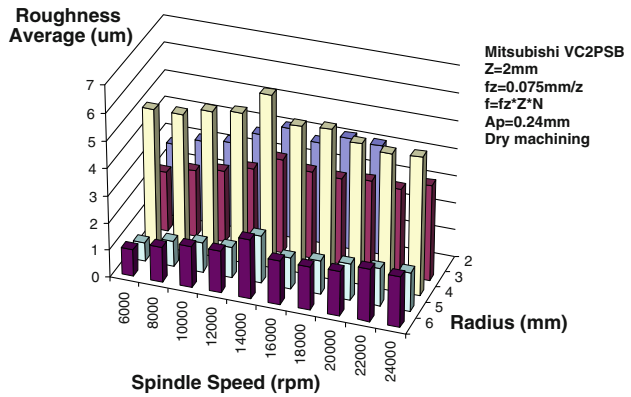

Fig. 11 Surface roughness average considering the cutting tool radius

and finally Fig. 11 presents the surface roughness obtained when the cutting tool radius is varied. On the right-hand side of these figures the rest of the process parameters selected for the series experiments are shown.

An artificial neural network model

All the data collected in the experimental stage of this work was used to feed and train an artificial neural network (ANN) for surface roughness predictions. An ANN is an interconnected group of artificial neurons arranged in several layers and linked through variable weights that uses a mathematical or computational model for information processing. These weights are calculated by means of an iterative method in the training process when the network is fed with training data. They can be used to model complex relationships between inputs and outputs or to find patterns in data, making the network a useful predictor of surface roughness generation.

Network accuracy and efficiency depend on various parameters such as hidden nodes, activation functions, training algorithm parameters and characteristics such as normalization and generalization. The number of hidden layers and the number of neurons in the hidden layers play an important role in the performance of the ANN. Using too few neurons in the hidden layers can lead to underfitting problems, which means that the network cannot provide good approximations. Conversely, the use of too many neurons in the hidden layers can result in overfitting problems as well as an unusual increase in training time. Overfitting or overtraining leads to a loss in generalization ability, as the training set is learned too specifically. A trade-off between too many and too few neurons in the hidden layers must be reached to get the most out of the neural network approach (Dewes and Aspinwall 1997). There is no well established procedure for finding the correct number, and most researchers employ a trial and error procedure. This research work tests and trains several networks. The neural network structure was built with the MATLAB^{TM} Neural Network Toolbox.

Three kinds of samples were used to train, validate and test the neural networks. Of the 250 samples corresponding to the experiments, 70%, or a total of 175, were randomly divided into training samples and introduced during the training, and the network was adjusted according to the error; 15%, or 38, were divided into validation samples and used to measure network generalization and to stop the training when the generalization stopped improving; and another 15%, or 37, had no effect on training and so provided an independent measure of the network's performance.

After several network configuration attempts using a trial and error procedure, the network that obtained the best correlation values was saved. The network architecture was a typical two-layer feed-forward network that was trained to followed a Levenberg-Marquardt backpropagation 'trainlm' algorithm. This training automatically stops when generalization stops improving, as indicated by an increase in the mean square error of the validation samples. One hidden layer with 20 neurons was used. The transfer function of the hidden layer was the tan-sigmoid 'tansig' and 'purelin' was the linear transfer function for the output layer. The learning function for weight and bias was 'learngdm', a learning function featuring gradient descent and momentum, weight and bias learning. Input arrays were processed with three functions: first, with 'fixunknowns' to process those rows with unknown

values and avoid the problems that Not Available Numbers (NaN) can entail; then, with 'removeconstantrows' to process the input matrix by removing rows with constant values that would not provide relevant information to the network; and finally, with a 'mapminmax' function to process the input matrix by normalizing the minimum and maximum values to [−1, 1]. Once again the output processing functions were 'removeconstantrows' and 'mapminmax'.

The output or target was surface roughness (Ra). The selection of the inputs was made with the aim of introducing a realistic view of the cutting process in the ANN. Inputs are composed by:

a) Process parameters: radial depth of cut (Ae); axial depth of cut (Ap); spindle speed (N); feed rate (f).
b) Deterministic process parameters: feed per tooth (fz); cutting speed (Vc); tooth passing frequency (ft); surface crest height (h); theoretical Ra (Rat); cutting section (Cs); material removal rate (MRR); power required (P).
c) Cutting tool characteristics: cutter radius (R); number of teeth (Z); wear (W); overhang (O).
d) Use of lubricants: dry machining or MQL.
e) Material properties: power coefficient (K); hardness (H).
f) Vibrations captured by accelerometers in the X and Y axes: low frequency vibration amplitude in the X and Y axes (lx, ly); medium frequency vibration amplitude in the X and Y axes (mx, my); high frequency vibration amplitude in the X and Y axes (hx, hy); temporal domain vibration amplitude in the X and Y axes (tdx, tdy); tooth passing frequency amplitude in the X and Y axes (tpx, tpy).

Deterministic process parameters are those cutting factors that can be calculated through formulae. Formulae to calculate fz, Vc and ft are widely known. The other deterministic process parameters specified (h, Rat, Cs, MRR and P) can be calculated with:

$$h = R - \frac{\sqrt{4R^2 - \mathrm{Ae}^2}}{2} \tag{3}$$

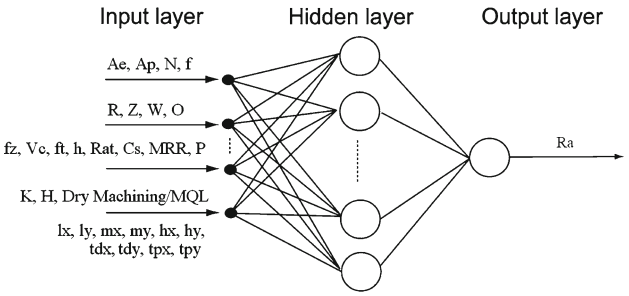

Fig. 12 Architecture of the artificial neural network used for surface roughness predictions

$$\mathrm{MRR} = f \times \mathrm{Cs}$$

$$\mathrm{MRR} = f\left[\left[\mathrm{Ae}\cdot\mathrm{Ap}\right] - \left[\mathrm{Ae}\cdot R - \frac{\mathrm{Ae}}{2}\left[\sqrt{R^2 - \left(\frac{\mathrm{Ae}}{2}\right)^2}\right] - R^2\cdot\sin^{-1}\left[\frac{\mathrm{Ae}}{2\cdot R}\right]\right]\right] \tag{5}$$

$$P = \mathrm{MRR}\times K \tag{6}$$

The power coefficient (K) can be obtained in López et al. (2008) and the hardness of the material (H) is given by the raw material provider. With regard to the vibration treatment, low frequencies are those lower than 500 Hz that capture, if they occur, vibrations due to machine-tool structure mode excitations (usually around 200 Hz). Medium frequencies are those between 500 and 2,500 Hz, as excitation of the system modes related to the spindle, the tool-holder and the cutting tool are typically around 2,000 Hz (Quintana et al. 2009). High frequencies are those between 2,500 and 5,000 Hz, as the maximum frequency at which the signal frequencies can be identified, according to the Nyquist-Shannon sampling theorem, is fs/2. Figure 12 shows the architecture of the neural network developed at this stage of the investigation.

$$\mathrm{Ra} = \frac{2}{\mathrm{Ae}}\left[R^2\cdot\cos^{-1}\left[\frac{\sqrt{R^2-\frac{\mathrm{Ae}^2}{4}}}{2R}+\frac{R}{\mathrm{Ae}}\sin^{-1}\left[\frac{\mathrm{Ae}}{2R}\right]\right]-\left[\frac{R^2}{\mathrm{Ae}}\cdot\sin^{-1}\left[\frac{\mathrm{Ae}}{2R}\right]+\frac{\sqrt{R^2-\frac{\mathrm{Ae}^2}{4}}}{2}\right]\right.$$
$$\left.\cdot\sqrt{-\frac{2R^3}{\mathrm{Ae}}\cdot\sin^{-1}\left[\frac{\mathrm{Ae}}{2R}\right]+2R^2-R\sqrt{R^2-\frac{\mathrm{Ae}^2}{4}}-\left[-\frac{R^2}{\mathrm{Ae}}\sin^{-1}\left[\frac{\mathrm{Ae}}{2R}\right]+R-\frac{\sqrt{R^2-\frac{\mathrm{Ae}^2}{4}}}{2}\right]^2}\right] \tag{4}$$

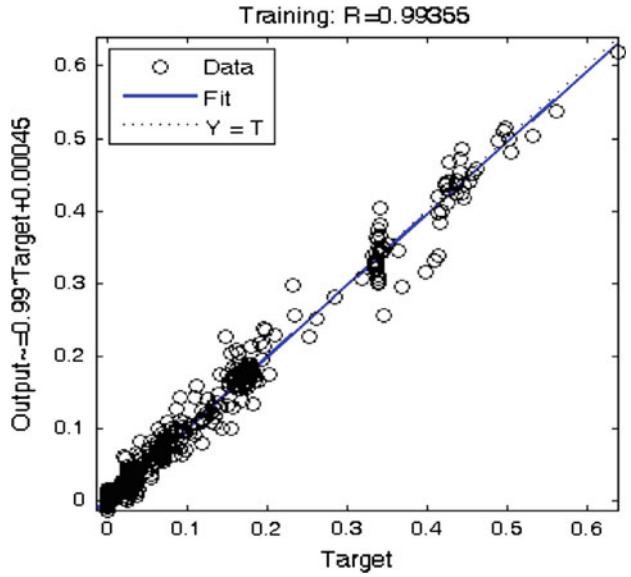

Fig. 13 Regression plot and correlation value (R) for the training samples

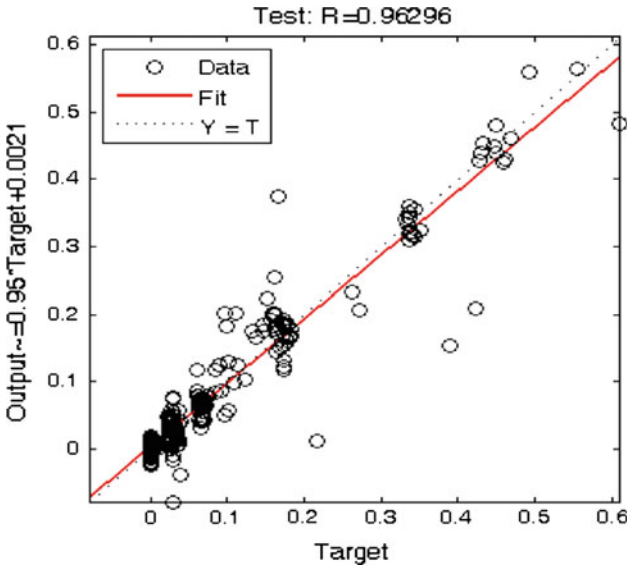

Fig. 15 Regression plot and correlation value (R) for the testing samples

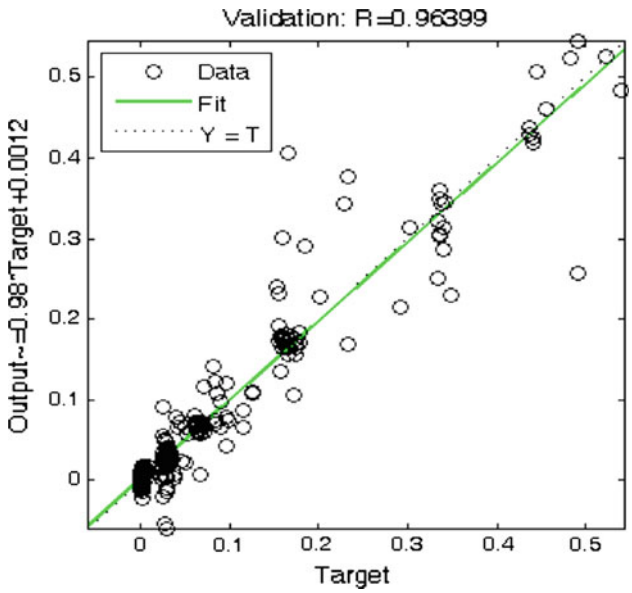

Fig. 14 Regression plot and correlation value (R) for the validation samples

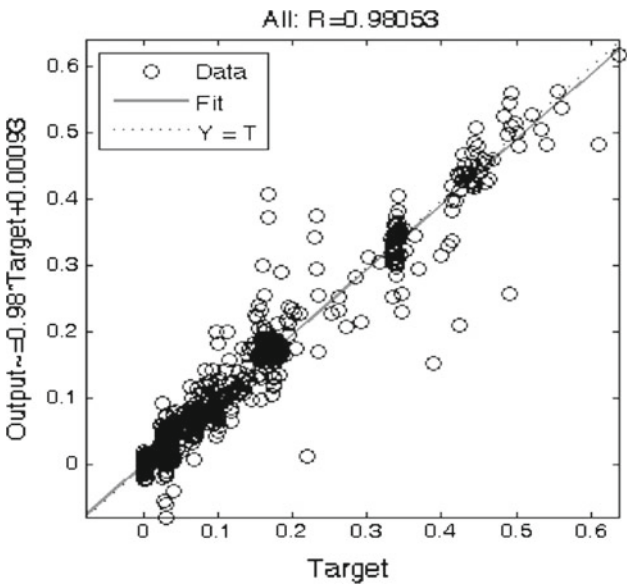

Fig. 16 Regression plot and correlation value (R) of the neural network model

The results provided by the ANN developed are clearly accurate, as can be seen from the high correlation values (R) in Figs 13, 14, 15 and 16. Regression (R) values measure the correlation between outputs and targets. Figure 13 shows the correlation value for the training sample ($R = 0.99355$) with the mean squared error (MSE = 0.000270). Figure 14 shows the correlation value obtained for the validating sample ($R = 0.96399$) with the mean squared error (MSE = 0.00058027). Figure 15 presents the correlation value for the testing sample ($R = 0.96296$) and Fig. 16 shows the fitting correlation of the entire surface roughness prediction model ($R = 0.98053$).

Monitoring model implementation

The surface roughness monitoring application was implemented as an interface combining LABVIEW^{TM} and MATLAB^{TM}. LABVIEW^{TM} was used to build a platform to capture the vibration and read the cutting parameters introduced by the user. MATLAB^{TM} was used to calculate surface roughness by applying the neural network developed once all the data had been introduced by the user and when the vibrations had been captured on line. The software is also capable of giving the surface roughness in line with the ISO

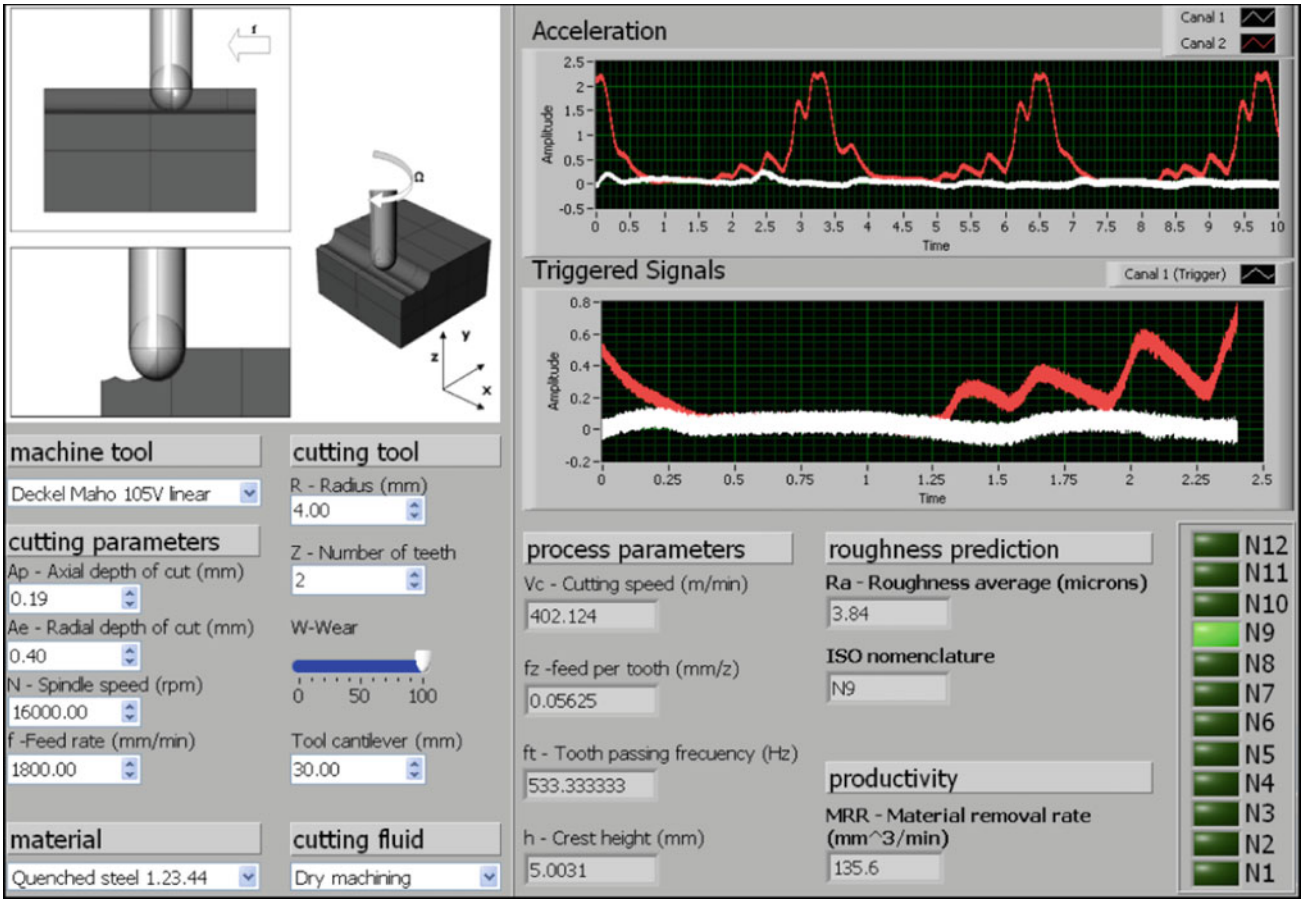

Fig. 17 Surface monitoring application main screen

Table 3 Surface roughness levels

ISO 1302:1996			
N12	50 μm	N6	0.80 μm
N11	25 μm	N5	0.40 μm
N10	12.5 μm	N4	0.20 μm
N9	6.30 μm	N3	0.10 μm
N8	3.20 μm	N2	0.050 μm
N7	1.60 μm	N1	0.025 μm

1302:1996 ranges that establish 12 levels from 0.006 to 50 μm, as shown in Table 3. In finish milling operations typical surface roughness levels vary from N6 to N9.

The main screen of the software used is shown in Fig. 17. The operator introduces the parameters required on the left side of the screen and the model calculates several process parameters, such as the cutting speed (Vc), the feed per tooth (mm/z), the tooth passing frequency (ft), the theoretical crest height (h) and also the productivity of the operation evaluated in terms of material removal rate (MRR). On the right side of the screen it provides online surface roughness predictions calculated with the artificial neural network developed, and, as previously mentioned, are also classified according to ISO levels. To perform the roughness calculations it is necessary to cut the vibration signals in order to extract only the vibration occurring when the cutter is effectively immersed in the part generating surface. Rapid traverses are removed on line with a trigger block. The vibrations captured with the two unidirectional accelerometers placed in the machine tool enclosure are also shown on the software screen (Fig. 17) on the right top side. Under this chart can be observed the triggered signal that has been cut in order to obtain the vibration that occurs when the cutting tool is machining the workpiece effectively. With the triggered vibration signal and the parameters introduced by the operator, surface roughness is calculated on line, while the part is in process. An example of the use of the software is shown in ASCAMM Technology Centre.

Conclusions

Surface roughness has a considerable influence on the performance of a finished part. It is a characteristic that is

usually evaluated out-of-process when the part is already machined and it is no longer possible to remove the defective part from the production chain. Roughness average (Ra) is a surface parameter that is often associated with quality.

Recent innovations and improvements in computers and sensors permit online process information to be obtained that can be used in monitoring. In this paper, a reliable surface roughness monitoring application based on an artificial neural network approach for vertical high speed milling operations has been presented. The model has been characterized for ball end mill finishing operations.

Experiments to obtain enough data to feed and train the ANN for surface roughness prediction were performed. The ANN was designed with a typical feedforward two-layer architecture. The selection of the inputs ensured a realistic introduction of cutting process characteristics in the ANN. Several different parameters were considered, such as process parameters, deterministic inputs, characteristics of the cutting tool, the use of lubricants, material properties and the vibrations that occur. Deterministic inputs and a detailed analysis of the vibration occurring during experimentation also permitted an increase in the accuracy of the approach presented. In addition, the extensive number of experiments carried out increased software performance by training of the network on the basis of a large amount of experience.

The next step in this research should be to develop an adaptive control system to modulate on line the surface roughness of the part in process and to ensure the desired level of quality while increasing productivity in terms of material removal rate.

A new model would be necessary to implement the ANN in other milling centers. As each machine tool behaves and performs differently, it would first be necessary to repeat the experiments to obtain information about the tool. To reduce the number of experiments required it could be advantageous to study the parameters typically used in finishing operations with the milling center being evaluated. Also, other materials or other types of tools could be incorporated into the monitoring application performing the required experimentation and retraining the ANN.

It is also possible to extend this methodology to study other types of machine tools, processes and technologies. In addition, the use of other sensors and monitoring technologies could be analyzed.

Acknowledgments The authors would like to express their gratitude to Javier Díaz for his technical contribution in the preliminary stages of this work, and to Marco Leonesio from ITIA (Istituto di Tecnologie Industriali e Automazione) for his interest and motivating technical observations. This research has been made possible by the financial support provided by NEXT Generation Production Systems, Integrated Project IP 011815, and the collaboration of partners.

References

Abouelatta, O. B., & Mádl, J. (2001). Surface roughness prediction based on cutting parameters and tool vibrations in turning operations. *Journal of Materials Processing Technology, 118*(1–3), 269–277.

ASCAMM Technology Centre, *cutOPT.* http://www.youtube.com/watch?v=v5nJZodMemY.

Benardos, P. G., & Vosniakos, G. (2003). Predicting surface roughness in machining: a review. *International Journal of Machine Tools and Manufacture, 6*:43(8):833–844.

Brezocnik, M., & Kovacic, M. (2003). Integrated genetic programming and genetic algorithm approach to predict surface roughness. *Materials and Manufacturing Processes, 18*(3), 475–491.

Brinksmeier, E., Aurich, J. C., Govekar, E., Heinzel, C., Hoffmeister, H., & Klocke, F., et al. (2006). Advances in modeling and simulation of grinding processes. *CIRP Annals-Manufacturing Technology, 55*(2), 667–696.

Chang, H., Kim, J., Kim, I. H., Jang, D. Y., & Han, D. C. (2007). In-process surface roughness prediction using displacement signals from spindle motion. *International Journal of Machine Tools and Manufacture, 47*(6), 1021–1026.

Chen, J. C., & Lou, M. S. (2000). Fuzzy-nets based approach to using an accelerometer for an in-process surface roughness prediction system in milling operations. *International Journal of Computer Integrated Manufacturing, 13*(4), 358–368.

Chukwujekwu Okafor, A., & Adetona, O. (1995). Predicting quality characteristics of end-milled parts based on multi-sensor integration using neural networks: individual effects of learning parameters and rules. *Journal of Intelligent Manufacturing, 6*(6), 389–400.

Ciurana, J., Arias, G., & Ozel, T. (2009). Neural network modeling the influence of process parameters on feature geometry and surface quality in pulsed laser micro-machining of hardened AISI H13 steel. *Materials and Manufacturing Processes, 24*(3), 1–11.

Correa, M., Bielza, C., & Pamies-Teixeira, J. (2009). *Comparison of Bayesian networks and artificial neural networks for quality detection in a machining process.* Expert systems with applications.

Correa, M., Bielza, C., Ramirez, M. D. J., & Alique, J. R. (2008). A Bayesian network model for surface roughness prediction in the machining process. *International Journal of Systems Science, 39*(12), 1181–1192.

Dewes, R. C., & Aspinwall, D. K. (1997). A review of ultra high speed milling of hardened steels. *Journal of Materials Processing Technology, 69*(1–3), 1–17.

Ghani, A. K., Choudhury, I. A., & Husni (2002). Study of tool life, surface roughness and viberation in machinning nodular cast iron with ceramic tool. *Journal of Materials Processing Technology, 127*(1), 17–22.

Grzesik, W. (2008). Influence of tool wear on surface roughness in hard turning using differently shaped ceramic tools. *Wear, 265*(3–4), 327–335.

Groover, M. P. (2004). *Society of manufacturing engineers. Fundamentals of modern manufacturing: Materials processes and systems* (2nd ed.). New York: Wiley.

Huang, B., & Chen, J. C. (2003). An in-process neural network-based surface roughness prediction (INN-SRP) system using a dynamometer in end milling operations. *International Journal of Advanced Manufacturing Technology, 21*(5), 339–347.

López, de., Lacalle, L. N., & Lamikiz A. (Eds.). (2008). *Machine Tools for High Performance Machining*

Markopoulos, A. P., Manolakos, D. E., & Vaxevanidis, N. M. (2008). Artificial neural network models for the prediction

of surface roughness in electrical discharge machining. *Journal of Intelligent Manufacturing, 19*(3), 283–292.

Martellotti, M. E. (1941). An analysis of the milling process. *Transactions of ASME, 63*, 667.

Martellotti, M. E. (1945). An analysis of the milling process. Part II: Down milling. *Transactions of ASME, 67*, 233–649.

Quintana, G., Ciurana, J., Ferrer, I., & Rodríguez, C. A. (2009). Sound mapping for identification of stability lobe diagrams in milling processes. *International Journal of Machine Tools and Manufacture, 49*(3–4), 203–211.

Quintana, G., Ribatallada, J., & Ciurana, Q. (2010). Surface roughness generation and material removal rate in ball end milling operations. *Materials and manufacturing processes. (In press).*

Risbood, K. A., Dixit, U. S., & Sahasrabudhe, A. D. (2003). Prediction of surface roughness and dimensional deviation by measuring cutting forces and vibrations in turning process. *Journal of Materials Processing Technology, 132*(1–3), 203–214.

Samanta, B., Erevelles, W., & Omurtag, Y. (2008). Prediction of workpiece surface roughness using soft computing. *Proceedings of the Institution of Mechanical Engineers. Part B: Journal of Engineering Manufacture, 222*(10), 1221–1232.

Sharma, V. S., Dhiman, S., Sehgal, R., & Sharma, S. K. (2008). Estimation of cutting forces and surface roughness for hard turning using neural networks. *Journal of Intelligent Manufacturing, 19*(4), 473–483.

Thomas, M., Beauchamp, Y., Youssef, A. Y., & Masounave, J. (1996). Effect of tool vibrations on surface roughness during lathe dry turning process. *Computers & Industrial Engineering, Elsevier, 31*(3/4), 637–644.

Tsai, Y., Chen, J. C., & Lou, S. (1999). An in-process surface recognition system based on neural networks in end milling cutting operations. *International Journal of Machine Tools and Manufacture, 39*(4), 583–605.

Zhang, J. Z., Chen, J. C., & Kirby, E. D. (2007). The development of an in-process surface roughness adaptive control system in turning operations. *Journal of Intelligent Manufacturing, 18*(3), 301–311.